Int J Wireless Inf Networks (2008) 15:53–60
DOI 10.1007/s10776-008-0073-x

LETTER

Error Probability Distribution and Density Functions for Rayleigh and Rician Fading Channels with Diversity

Chen Jie · Vidhyacharan Bhaskar

Published online: 6 March 2008

Abstract This paper analyzes the distribution and density functions of the probability of error for Rayleigh and Rician fading channels with diversity. An expression for the signal-to-noise ratio is derived for an asynchronous CDMA (A-CDMA) system with diversity. The error probability distribution and density functions are derived and plotted for different mean energy-to-noise ratios.

Keywords Error probability distribution and density functions · Diversity · Rayleigh fading · Rician fading

1 Introduction

In this work, we derive the error probability distribution and density functions to characterize the fading process in an asynchronous CDMA (A-CDMA) system. Rayleigh and Rician slow fading channels are considered in this paper. The fading process can be obtained by considering the mean-square values of the signal and noise. The distribution and density functions are useful in defining the "fading margin" used to accommodate the expected amount of fading to maintain the Quality of Service (QoS) for the given type of traffic in the channel.

C. Jie
Department of Information systems and Telecommunications, University of Technology of Troyes, Troyes, France

V. Bhaskar (✉)
Department of Electronics and Communication Engineering, SRM University, Kattankulathur, Kancheepuram Dt. 603203, Tamilnadu, India
e-mail: meetvidhyacharan@yahoo.com

Rayleigh fading has been shown to convert an exponential dependency of the bit error probability (BEP) on the signal-to-noise ratio (SNR) into an inverse linear one, thereby resulting in a very large SNR penalty. Diversity technique is a very effective remedy that exploits the principle of providing the receiver with multiple faded replicas of the same information bearing signal [1].

In [2], an accurate analytical solution for the bit error rate (BER) of a DS-CDMA system operating over Rayleigh fading channels has been derived. In addition to this, a new closed-form expression is provided for the characteristic function of the interfering signals. Choe et al. in [3] employ the transfer function approach to obtain error probability upper bounds for asynchronous trellis-coded CDMA systems based on biorthogonal signature sequences. This technique provides uniformly tight bounds for the biorthogonal sequence based trellis codes, both with and without parallel transitions.

In [4], the BER performance of a two-dimensional (2-D) RAKE receiver in combination with transmit diversity on the downlink of a wideband CDMA (W-CDMA) system, is presented. In addition, the exact pairwise error probability of a convolutional coded system is obtained, and the coding gain of a space-path diversity receiver is quantified. Wei and Jana in [5] estimate the BER of optimum multiuser detection for synchronous and asynchronous CDMA systems on additive white Gaussian and fading channels. Upper and lower bounds on the BER for a given spreading code are also computed.

Zhang et al. in [6] study the behavior of the output multiple access interference (MAI) of the minimum mean-square error (MMSE) receiver employed in the uplink of a direct sequence CDMA (DS-CDMA) system. They extend their study to asynchronous systems and establish the additive white Gaussian nature of the output interference. The Gaussianity

justifies the use of a single-user, multiple-interferer CDMA system with linear MMSE receiver, and from the view points of detection and channel capacity, signal-to-interference (SIR) ratio is the key parameter that governs the performance of an MMSE receiver in a CDMA system.

In [7], modulation schemes like M-ary phase-shift keying and differential phase-shift keying (DPSK) on a slow fading Rayleigh channel without diversity, are investigated. Closed-form expressions for the distribution of the phase angle between a vector with Rayleigh amplitude distribution and a noiseless reference, and between two vectors both with Rayleigh amplitude distribution perturbed by additive white Gaussian noise are obtained.

A unified approach to determine the exact BER of noncoherent and differentially coherent modulations with single and multichannel receptions over additive white Gaussian noise and generalized fading channels, is presented in [8]. The multichannel reception results assume independent fading in the channels and are applicable to systems that employ post-detection equal gain combining.

Bithas et al. study the performance of switch and stay combining (SSC) diversity receivers operating over correlated Rician fading satellite channels in [9]. An infinite series representation for the bivariate Rician probability density function, and the density function of the SSC output signal-to-noise ratio are derived. Analytical expressions for the cumulative distribution function, moments of output SNR, moment generating function and average channel capacity are derived.

A new technique for determining the probability of error of a general equal gain combiner (EGC) over Rayleigh fading channels is presented in [10]. This new technique takes a single step and directly derives the error performance from the characteristic function of the decision variable, thereby avoiding the lengthy process of deriving the distribution of the sum of Rayleigh variates and eliminating all approximations required therein.

In [11], a generalized compound fading model which takes into account both fading and shadowing in wireless system is presented. The compound probability density function (pdf) developed in [11] is analytically simpler than the two pdfs based on lognormal shadowing, and is general enough to incorporate most of the fading and shadowing observed in wireless channels. Ma et al. in [12] discuss the performance of communication systems using binary coherent and DPSK modulation in correlated Rician fading channels with diversity reception. Exact BER expressions are derived via the moment generating functions (MGFs) of the relevant decision statistics, which are obtained through coherent detection with equal gain combining for differential modulation.

In [13], the error performance of non-coherent detection receivers for FSK signals transmitted over fast frequency-flat Rician fading channels is computed. Error bounds are established for the performance of M-ary orthogonal FSK. Ugweje proposes and analyzes a multicarrier CDMA system with application to image signal transmission in [14]. The image signal is partitioned into subsets and a different subband carrier modulates each subset. The BER is evaluated in the presence of multipath fading, thermal noise and is a function of data rate, bandwidth, delay range, and space diversity.

The work carried out in [15] presents a method for the approximation of the BER probability density function of asynchronous multicarrier code division multiple access (MC-CDMA) and DS-CDMA systems. This method is applicable for any given set of spreading codes. The MC-CDMA scheme is found to offer higher MAI resistance than conventional DS-CDMA in an asynchronous environment for the Walsh Hadamard and Gold codes considered.

A new practical technique for determining the bit error rate of multiuser MC-CDMA systems in frequency-selective Nakagami-*m* fading channels is presented in [16]. The analysis assumes that different subcarriers experience independent fading channels which are not necessarily identically distributed.

The performance of CDMA in the case of imperfect power control is discussed in [17]. An extension to [17] is investigated in [18], wherein the error probability of a multi-cell CDMA system operating with imperfect power control over a frequency-selective multipath fading channel is derived. It is found that the effect of power control error is decreased by using diversity combining techniques.

This paper is an extension of a previous paper published by Bhaskar et al. in [19], where the authors have considered the distribution and density functions of the probability of error in Rayleigh and Rician fading channels with no diversity. For identical values of signal-to-noise ratio, diversity combining is expected to yield lower probability of bit error than that obtained without diversity. Thus, the cumulative distribution function peaks faster for the diversity combining case as compared to the no diversity case. The peak values of the density function, which denote the relative frequency of error occurrence, is lower for the case with diversity combining as compared to the no diversity case. This work is different from [19] since it employs diversity for the fading channels, and then computes the distribution function of the probability of error, and its relationship with the distribution function of the signal energy-to-noise ratio for fading channels with diversity.

Section 2 provides the block diagram and description of the A-CDMA system incorporating diversity for the fading channels and derives an expression for the signal-to-noise ratio in fading channels with diversity. Section 3 provides a detailed mathematical analysis of error probability

distribution and density functions for Rayleigh and Rician fading channels with diversity. Section 4 plots the distribution and density functions of the probability of error, and discusses the numerical results. Finally, Sect. 5 presents the conclusions.

2 System Description

In this paper, uplink (mobile users to base station) channels are considered. The block diagram shown in Fig. 1 is that of a single-user, multiple-interferer A-CDMA system with L diversity receiver antennas for L fading channels for the desired user (user 0). Of the U users, there is one desired user and $(U-1)$ undesired users (interferers). Each path in which the signal traverses from the desired user to each receiver antenna is a fading channel. The fading is considered to be either Rayleigh or Rician. The multiple user system can be considered as a single-user, multiple-interferer system if the total effect of the $(U-1)$ interferers is approximately Gaussian. This approximation is valid if the sum of the interferer powers are non negligible compared to the power of user 0. At the receiver side, the total received signal can be expressed in the form

$$r(t) = x_0(t) + I_{U-1}(t) + n(t), \tag{1}$$

where $(U-1)$ is the number of interferers, $x_0(t)$ is the received signal of the desired user (user 0), $I_{U\text{-}1}(t) = x_1(t) + \ldots + x_{U\text{-}1}(t)$ is the interference term and $n(t)$ is the thermal noise.

Suppose for each fading channel, the impulse response is $h_0^{(i)}(t)$, $1 \le i \le L$. Then, the received signal from user 0 is

$$x_0(t) = s_0(t) * \sum_{i=1}^{L} h_0^{(i)}(t), \tag{2}$$

where $s_0(t) = \sqrt{2P_0}a_0(t)b_0(t)\cos(\omega_c t)$, and * denotes the convolution operation.

Here,

- P_0 is the transmitted signal power of user 0,
- $a_0(t)$ is the pseudo random spreading code of user 0,
- $b_0(t)$ is the information signal of user 0,
- $\cos(\omega_c t)$ is the carrier signal for user 0, where ω_c is expressed in radians per second.

Similarly, the received signals from the undesired users, users 1, 2, ..., $(U-1)$, are

$$\begin{aligned} x_1(t) &= \sqrt{2P_1}a_1(t-\delta_1)b_1(t-\delta_1)\cos(\omega_c t+\phi_1) * \sum_{i=1}^{L} h_1^{(i)}(t), \\ &\vdots \\ x_{U-1}(t) &= \sqrt{2P_{U-1}}a_{U-1}(t-\delta_{U-1})b_{U-1}(t-\delta_{U-1}) \\ &\quad \times \cos(\omega_c t+\phi_{U-1}) * \sum_{i=1}^{L} h_{U-1}^{(i)}(t), \end{aligned} \tag{3}$$

where

- P_i is the transmitted signal power of undesired user i, $1 \le i \le U-1$,
- $a_i(t)$ is the pseudo random spreading code of undesired user i,
- $b_i(t)$ is the information signal of undesired user i,
- δ_i is the user delay of undesired user i,
- ϕ_i is the phase shift of undesired user i,
- $h_j^{(i)}(t)$ is the impulse response of the i^{th} fading channel of the j^{th} undesired user, $1 \le j \le U-1$.

Assume that the multipath fading channels are Rayleigh or Rician distributed. Let $A_k(t)$ be the received signal amplitude for user k, and $\Phi_k(t)$ be the phase shift of the kth

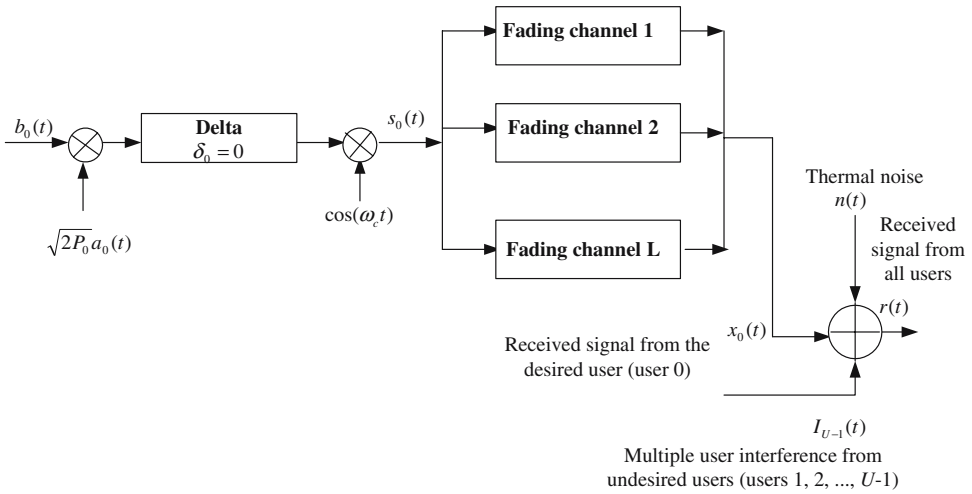

Fig. 1 Block diagram of the A-CDMA system with L receiver antennas

user due to the slow fading channel. For a slow fading channel, $A_k(t)$ and $\Phi_k(t)$ can be assumed to be a constant over a symbol duration T. If $A_k^{(i)}(t)$ and $\theta_k^{(i)}(t)$ are the amplitude and phase shift of the received signal from user k and fading channel i, we can write $s_k(t-\delta_k)*\sum_{i=1}^{L} A_k^{(i)}(t)e^{j\theta_k^{(i)}(t)} = A_k(t)e^{j\Phi_k(t)}$. The received signal from the kth user is

$$x_k(t-\delta_k) = \sqrt{2P_k}A_k(t)a_k(t-\delta_k)b_k(t-\delta_k)\cos(\omega_c t + \phi_k + \Phi_k(t)), \tag{4}$$

where the user delays, δ_k, are due to the asynchronous system, $A_k(t) = f(A_k^{(i)}(t), \theta_k^{(i)}(t), s_k(t-\delta_k), L)$, $\Phi_k(t) = h(A_k^{(i)}(t), \theta_k^{(i)}(t), s_k(t-\delta_k), L)$, and $f(.)$, $h(.)$ are functions of $A_k^{(i)}(t)$, $\theta_k^{(i)}(t)$, $s_k(t-\delta_k)$, and L.

The short-term mean-squared value of the received signal from all users neglecting noise can be expressed as

$$\begin{aligned}\langle x^2(t)\rangle &= \left\langle \left(\sum_{k=0}^{U-1} x_k(t-\delta_k)\right)^2 \right\rangle \\ &= \left\langle \left(\sum_{k=0}^{U-1} A_k(t)\sqrt{2P_k}a_k(t-\delta_k)b_k(t-\delta_k) \times \cos\left(\omega_c t + \phi_k + \Phi_k(t)\right)\right)^2 \right\rangle,\end{aligned} \tag{5}$$

where the $\langle . \rangle$ refers to the time-average over time period T. Rewriting it, we have

$$\begin{aligned}\langle x^2(t)\rangle &= \frac{1}{T}\int_0^T \left(\sum_{k=1}^{U-1} A_k(t)\sqrt{2P_k}a_k(t-\delta_k)b_k(t-\delta_k) \times \cos(\omega_c t + \phi_k + \Phi_k(t))\right)^2 dt \\ &= \frac{1}{T}\int_0^T \sum_{k=1}^{U-1}\sum_{l=1}^{U-1} A_k(t)A_l(t)2\sqrt{P_k P_l}a_k(t-\delta_k) \times a_l(t-\delta_l)b_k(t-\delta_k)b_l(t-\delta_l) \\ &\quad \times \cos(\omega_c t + \phi_k + \Phi_k(t))\cos(\omega_c t + \phi_l + \Phi_l(t))dt, \\ &= \frac{1}{T}\int_0^T \sum_{k=1}^{U-1}\sum_{l=1}^{U-1} A_k(t)A_l(t)\sqrt{P_k P_l}a_k(t-\delta_k) \times a_l(t-\delta_l)b_k(t-\delta_k)b_l(t-\delta_l) \\ &\quad \times [\cos(\phi_k - \phi_l + \Phi_k(t) - \Phi_l(t)) + \cos(2\omega_c t + \phi_k + \phi_l + \Phi_k(t) + \Phi_l(t))]dt.\end{aligned} \tag{6}$$

For $\omega_c \gg T^{-1}$, (6) can be approximated as

$$\begin{aligned}\langle x^2(t)\rangle &\approx \frac{1}{T}\sum_{k=1}^{U-1}\sum_{l=1}^{U-1}\sqrt{P_k P_l}\int_0^T a_k(t-\delta_k) \\ &\quad \times a_l(t-\delta_l)b_k(t-\delta_k)b_l(t-\delta_l) \\ &\quad \times \cos(\phi_k - \phi_l + \Phi_k(t) - \Phi_l(t))dt,\end{aligned} \tag{7}$$

since the received signal amplitudes, $A_k(t)$ and $A_l(t)$ of the kth and the lth users respectively are assumed to be a constant over symbol duration T. If the aperiodic cross-correlations of the spreading sequences are small, (7) can be approximated as

$$\begin{aligned}\langle x^2(t)\rangle &\approx \sum_{k=1}^{U-1} A_k^2(t)P_k \\ &= \sum_{k=1}^{U-1}\left(f(A_k^{(i)}(t), \theta_k^{(i)}(t), s_k(t-\delta_k), L)\right)^2 P_k.\end{aligned} \tag{8}$$

The short-term mean-squared value of noise can be expressed as $\langle n^2(t)\rangle \approx N_0 W_n = N_P$, where N_0 is the single-sided noise spectral density, W_n is the system bandwidth in Hz, and N_P is the detected noise power. Thus, the signal-to-noise ratio is

$$\begin{aligned}\mathrm{SNR}(t) &= \frac{\langle x^2(t)\rangle}{\langle n^2(t)\rangle} \\ &= \frac{\sum_{k=1}^{U-1}\left(f\left(A_k^{(i)}(t), \theta_k^{(i)}(t), s_k(t-\delta_k), L\right)\right)^2 P_k}{N_0 W_n}.\end{aligned} \tag{9}$$

3 Error Probability Distribution and Density Functions

To characterize the fading process in a communication system, error probability performance in a fading environment is used to calculate the probability of error averaged over the additive noise and signal-fading distributions.

The probability of error, $P_e(t)$ is a random process, which depends on the fading of the signal. The probability of error can be expressed as a function of the energy-to-noise ratio [20]

$$P_e(t) = g\left[\frac{E(t)}{N_0}\right], \tag{10}$$

where $E(t)$ represents the detected signal energy variations due to signal fading. The function $g(x)$ depends on the type of modulation scheme used.

Substituting (9) into (10) (where SNR(t) is proportional to $\frac{E(t)}{N_0}$ with proportionality constant $\frac{1}{W_n}$), we have

$$P_e(t) = g\left[\frac{\sum_{k=1}^{U-1}\left(f\left(A_k^{(i)}(t), \theta_k^{(i)}(t), s_k(t-\delta_k), L\right)\right)^2 P_k}{N_0 W_n}\right]. \tag{11}$$

3.1 Cumulative Distribution Function

The cumulative distribution function (CDF) of $P_e(t)$ is given by

$$\begin{aligned} F_{P_e(t)}(y) &= \mathrm{P}(P_e(t) \le y) = \mathrm{P}\left(\frac{E(t)}{N_0} \ge g^{-1}(y)\right) \\ &= 1 - \mathrm{P}\left(\frac{E(t)}{N_0} < g^{-1}(y)\right) \\ &= 1 - F_{\frac{E(t)}{N_0}}\left(g^{-1}(y)\right), 0 \le y \le \frac{1}{2} \end{aligned} \tag{12}$$

where $F_{\frac{E(t)}{N_0}}(g^{-1}(y))$ is the cumulative distribution function of the signal energy-to-noise variations. In (12), the inequality is reversed in the second step because $g\left[\frac{E(t)}{N_0}\right]$ is a decreasing function of $\frac{E(t)}{N_0}$. Now, the detected signal energy-to-noise ratio, $\frac{E(t)}{N_0}$, is directly proportional to the SNR variations, which is in turn proportional to the square of the received signal amplitude. The proportionality factor is the transmitted signal energy-to-noise ratio, $R = \frac{B^2T}{N_0}$, where B represents the amplitude of the modulated signal, and T represents the symbol duration. In the case of coherent detection with automatic phase control (perfect carrier synchronization with the received modulated signal), we can write [20]

$$\frac{E(t)}{N_0} = \frac{Ra^2(t)}{2}, \tag{13}$$

where $a(t)$ is the amplitude of the fading on the received signal which has a density function that is Rayleigh or Rician distributed depending on the type of the fading channel. It should be noted that $\frac{E(t)}{N_0}$ has a chi-square (central) distribution if $a(t)$ is Rayleigh distributed, and a chi-square (non-central) distribution if $a(t)$ is Rician distributed. If $a(t)$ is Rayleigh distributed with L-fold diversity, letting $Y = \frac{E(t)}{N_0}$, we have

$$\begin{aligned} F^{(L)}_{\frac{E(t)}{N_0},\mathrm{RaF}}\left[g^{-1}(y)\right] &= F^{(L)}_{Y,\mathrm{RaF}}\left[g^{-1}(y)\right] \\ &= 1 - \exp\left[-\frac{g^{-1}(y)}{2\sigma^2}\right]\sum_{k=0}^{m-1}\frac{1}{k!}\left(\frac{g^{-1}(y)}{2\sigma^2}\right)^k, \end{aligned} \tag{14}$$

where $g^{-1}(y) \ge 0$. In (14), RaF stands for Rayleigh fading. If $a(t)$ is Rician distributed with L-fold diversity, we have

$$\begin{aligned} F^{(L)}_{\frac{E(t)}{N_0},\mathrm{RiF}}\left[g^{-1}(y)\right] &= F^{(L)}_{Y,\mathrm{RiF}}\left[g^{-1}(y)\right] \\ &= 1 - Q_m\left(\frac{s}{\sigma}, \frac{\sqrt{g^{-1}(y)}}{\sigma}\right), \end{aligned} \tag{15}$$

where Q_m is the Marcum's Q function of order m, $m = \frac{n}{2}$, and n is the number of degrees of freedom. Here, $n = L$. In (15), RiF stands for Rician fading. Substituting (15) into (12) and (14) into (12), we have

$$\begin{aligned} F^{(L)}_{P_e(t),\mathrm{RaF}}(y) &= 1 - F^{(L)}_{\frac{E(t)}{N_0},\mathrm{RaF}}\left(g^{-1}(y)\right) \\ &= \exp\left[-\frac{g^{-1}(y)}{2\sigma^2}\right]\sum_{k=0}^{m-1}\frac{1}{k!}\left(\frac{g^{-1}(y)}{2\sigma^2}\right)^k, \end{aligned} \tag{16}$$

and

$$F^{(L)}_{P_e(t),\mathrm{RiF}}(y) = 1 - F^{(L)}_{\frac{E(t)}{N_0},\mathrm{RiF}}\left(g^{-1}(y)\right) = Q_m\left(\frac{s}{\sigma}, \frac{\sqrt{g^{-1}(y)}}{\sigma}\right). \tag{17}$$

3.2 Density Function

Density function graph is analogous to a histogram graph. The density function amplitude denotes the relative frequency of occurrence of errors (number of times of error occurrence) for each value of $P_e(t)$.

3.2.1 Rayleigh Fading Case

In the Rayleigh fading case, the density function of $P_e(t)$ is given by

$$\begin{aligned} & f_{P_e(t),\mathrm{RaF}}(y) \\ &= \frac{\partial}{\partial y}F^{(L)}_{P_e(t),\mathrm{RaF}}(y) \\ &= \frac{\partial}{\partial y}\left\{\exp\left[-\frac{g^{-1}(y)}{2\sigma^2}\right]\sum_{k=0}^{m-1}\frac{1}{k!}\left(\frac{g^{-1}(y)}{2\sigma^2}\right)\right\} \\ &= \frac{\partial}{\partial g^{-1}(y)}\left\{\exp\left[-\frac{g^{-1}(y)}{2\sigma^2}\right]\sum_{k=0}^{m-1}\frac{1}{k!}\left(\frac{g^{-1}(y)}{2\sigma^2}\right)\right\}\frac{\partial g^{-1}(y)}{\partial y} \\ &= -\frac{1}{(2\sigma^2)^m\Gamma(m)}\left[g^{-1}(y)\right]^{m-1}\exp\left(-\frac{g^{-1}(y)}{2\sigma^2}\right)\frac{\partial g^{-1}(y)}{\partial y}. \end{aligned} \tag{18}$$

For a Rayleigh or Rician fading channel with L-fold diversity, probability of bit error is given by [1]

$$y = g(\gamma_c) = \left[\frac{1}{2}(1-\mu)\right]^L\sum_{k=0}^{L-1}\mathrm{C}_k^{L-1+k}\left[\frac{1}{2}(1+\mu)\right]^k, \tag{19}$$

where C_k^{L-1+k} is the number of combinations of $(L-1+k)$ things chosen k at a time, $\mu = \sqrt{\frac{\gamma_c}{1+\gamma_c}}$, and γ_c is the average SNR. Thus,

$$\begin{aligned} \frac{\partial y}{\partial \gamma_c} &= \frac{\partial}{\partial \mu}\left\{\left[\frac{1}{2}(1-\mu)\right]^L\sum_{k=0}^{L-1}\mathrm{C}_k^{L-1+k}\left[\frac{1}{2}(1+\mu)\right]^k\right\}\frac{\partial \mu}{\partial \gamma_c} \\ &= \left(\sum_{k=0}^{L-1}\mathrm{C}_k^{L-1+k}\left[\frac{1}{2}(1+\mu)\right]^k\frac{\partial}{\partial \mu}\left[\frac{1}{2}(1-\mu)\right]^L\right. \end{aligned}$$

$$+\left[\frac{1}{2}(1-\mu)\right]^{L}\frac{\partial}{\partial\mu}\left(\sum_{k=0}^{L-1}C_k^{L-1+k}\left[\frac{1}{2}(1+\mu)\right]^{k}\right)\frac{\partial\mu}{\partial\gamma_c}$$
$$=\left(-yL(1-\mu)^{-1}+\left[\frac{1}{2}(1-\mu)\right]^{L}\sum_{k=1}^{L-1}C_k^{L-1+k}\left(\frac{1}{2}\right)^{k}\times k(1+\mu)^{k-1}\right)\frac{\partial\mu}{\partial\gamma_c}. \quad (20)$$

But,

$$\frac{\partial\mu}{\partial\gamma_c}=\frac{1}{2}\left(\frac{\gamma_c}{1+\gamma_c}\right)^{-\frac{1}{2}}\frac{1}{(1+\gamma_c)^2}=\frac{(1-\mu^2)^2}{2\mu}.$$

Hence,

$$\frac{\partial y}{\partial\gamma_c}=\left(-yL(1-\mu)^{-1}+\left[\frac{1}{2}(1-\mu)\right]^{L}\sum_{k=1}^{L-1}C_k^{L-1+k}\times\left(\frac{1}{2}\right)^{k}k(1+\mu)^{k-1}\right)\frac{(1-\mu^2)^2}{2\mu}. \quad (21)$$

The density function of the probability of error for a Rayleigh fading channel with L-fold diversity is obtained by substituting the reciprocal of $\frac{\partial y}{\partial\gamma_c}$ in (21) for $\frac{\partial g^{-1}(y)}{\partial y}$ in (18).

3.2.2 Rician Fading Case

In the Rician fading case, the density function of $P_e(t)$ is given by

$$\begin{aligned}f_{P_e(t),\mathrm{RiF}}(y)&=\frac{\partial}{\partial y}F_{P_e(t),\mathrm{RiF}}(y)=\frac{\partial}{\partial y}Q_m\left(\frac{s}{\sigma},\frac{\sqrt{g^{-1}(y)}}{\sigma}\right)\\&=\frac{\partial}{\partial g^{-1}(y)}Q_m\left(\frac{s}{\sigma},\frac{\sqrt{g^{-1}(y)}}{\sigma}\right)\frac{\partial g^{-1}(y)}{\partial y}\\&=-f_{\frac{E(t)}{N_0},\mathrm{RiF}}\left(g^{-1}(y)\right)\frac{\partial g^{-1}(y)}{\partial y}\\&=-\frac{1}{2\sigma^2}\left(\frac{g^{-1}(y)}{s^2}\right)^{\frac{L-2}{4}}\exp\left(-\frac{s^2+g^{-1}(y)}{2\sigma^2}\right)\\&\quad\times I_{\frac{L}{2}-1}\left(\frac{s^2\sqrt{g^{-1}(y)}}{\sigma^2}\right)\frac{\partial g^{-1}(y)}{\partial y},\end{aligned} \quad (22)$$

where $s=\gamma\sqrt{2}\sigma^2$ and $I_{\frac{L}{2}-1}(.)$ is the modified Bessel function of order $\left(\frac{L}{2}-1\right)$. Here, s is the Rician fading term, γ is the Rician fading parameter, and $\sigma^2=\frac{N_0}{2}$ is the variance of the Gaussian random variables making up the Rayleigh and Rician distributions. The density function of the probability of error for a Rician fading channel with L-fold diversity is obtained by substituting the reciprocal of $\frac{\partial y}{\partial\gamma_c}$ in (21) for $\frac{\partial g^{-1}(y)}{\partial y}$ in (22).

4 Numerical results

Figure 2 shows the cumulative distribution function of the probability of error in a Rayleigh fading channel with 6-fold diversity for various mean values of the detected signal energy-to-noise variations, $\left\langle\frac{E(t)}{N_0}\right\rangle$. We choose $R=1$ in the discussion of distribution and density functions. For higher values of $\left\langle\frac{E(t)}{N_0}\right\rangle$, the distribution function reaches a maximum quicker than those with lower $\left\langle\frac{E(t)}{N_0}\right\rangle$. Thus, the peak value of the cumulative distribution function of the probability of error is higher for a system with larger $\left\langle\frac{E(t)}{N_0}\right\rangle$ as compared to a system with lower $\left\langle\frac{E(t)}{N_0}\right\rangle$. For higher values of $\left\langle\frac{E(t)}{N_0}\right\rangle$, the probability of achieving low probability of error is higher than the case with lower values of $\left\langle\frac{E(t)}{N_0}\right\rangle$. The distribution function peaks up quicker for higher values of $\left\langle\frac{E(t)}{N_0}\right\rangle$ because it can find large number of probability values which have low probability of error as compared to the case when $\left\langle\frac{E(t)}{N_0}\right\rangle$ is lower.

Figure 3 shows the cumulative distribution function of the probability of error in a Rician fading channel with 6-fold diversity for various mean values of $\left\langle\frac{E(t)}{N_0}\right\rangle$ with constant Gaussian variance, $\sigma^2=0.2$ and different γ. Again, for higher values of $\left\langle\frac{E(t)}{N_0}\right\rangle$, the distribution function reaches a maximum quicker than those with lower $\left\langle\frac{E(t)}{N_0}\right\rangle$. The sum of the probabilities of finding lower $P_e(t)$ is higher for a system with higher $\left\langle\frac{E(t)}{N_0}\right\rangle$ than for a system with lower $\left\langle\frac{E(t)}{N_0}\right\rangle$.

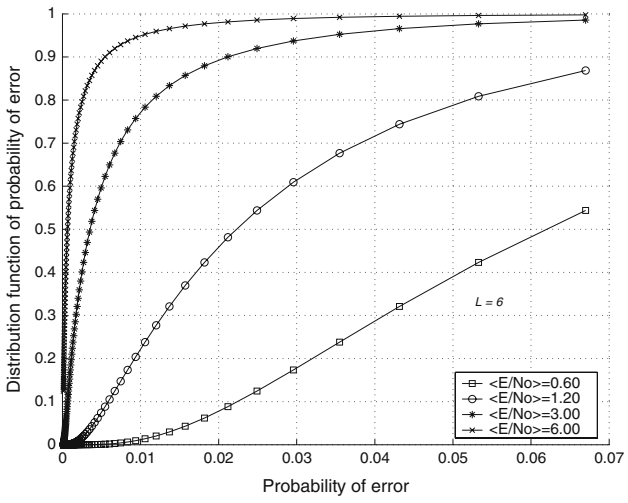

Fig. 2 Cumulative distribution function of the probability of error for a Rayleigh fading with 6-fold diversity for $\left\langle\frac{E(t)}{N_0}\right\rangle=0.6,1.2,3,6$, different variances

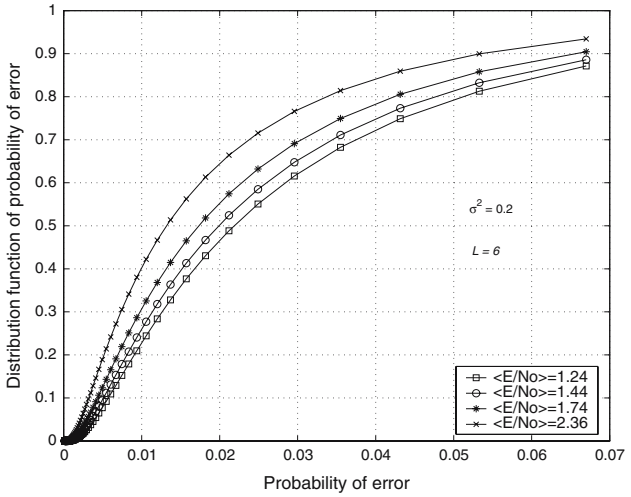

Fig. 3 Cumulative distribution function of the probability of error for a Rician fading with 6-fold diversity for $\left\langle \frac{E(t)}{N_0} \right\rangle = 1.24, 1.44, 1.74, 2.36$, different Rician fading parameters (γ), constant variance, $\sigma^2 = 0.2$

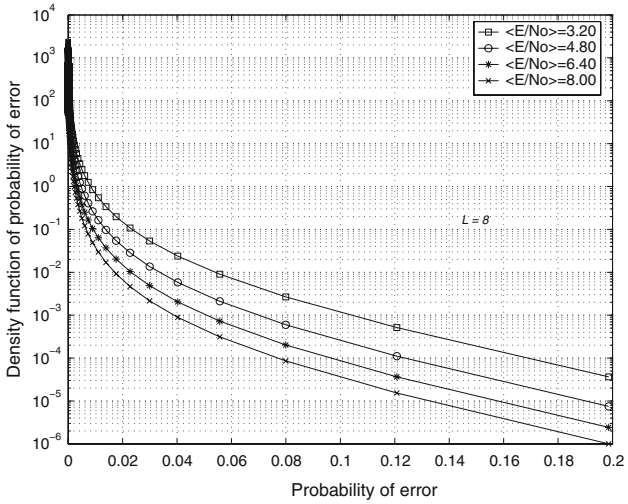

Fig. 5 Density function of the probability of error for a Rayleigh fading with 8-fold diversity for $\left\langle \frac{E(t)}{N_0} \right\rangle = 3.2, 4.8, 6.4, 8$, different variances

Figure 4 shows the cumulative distribution function of the probability of error in a Rician fading channel with 6-fold diversity for various mean values of $\left\langle \frac{E(t)}{N_0} \right\rangle$ with constant Rician fading parameter, $\gamma = 1.5$ and different σ^2. Higher values of σ^2 correspond to higher values of $\left\langle \frac{E(t)}{N_0} \right\rangle$, which would mean that the distribution function reaches a maximum quicker than those with lower $\left\langle \frac{E(t)}{N_0} \right\rangle$.

Figure 5 shows the density function of the probability of error in a Rayleigh fading channel with 8-fold diversity for various mean values of $\left\langle \frac{E(t)}{N_0} \right\rangle$ with different variances. The amplitude of the density function curves indicate the relative frequencies of the random variable, $P_e(t)$, occurring in the range $0 < P_e(t) < 0.2$. The frequencies are higher for a lower $\left\langle \frac{E(t)}{N_0} \right\rangle$, and lower for a higher $\left\langle \frac{E(t)}{N_0} \right\rangle$, which is expected.

Figure 6 shows the density function of the probability of error in a Rician fading channel with 8-fold diversity for various mean values of $\left\langle \frac{E(t)}{N_0} \right\rangle$ with constant variance, $\sigma^2 = 0.2$. Again, the relative frequencies of $P_e(t)$ occurring in the range $0 < P_e(t) < 0.08$, are higher for a lower $\left\langle \frac{E(t)}{N_0} \right\rangle$, and lower for a higher $\left\langle \frac{E(t)}{N_0} \right\rangle$, which is expected.

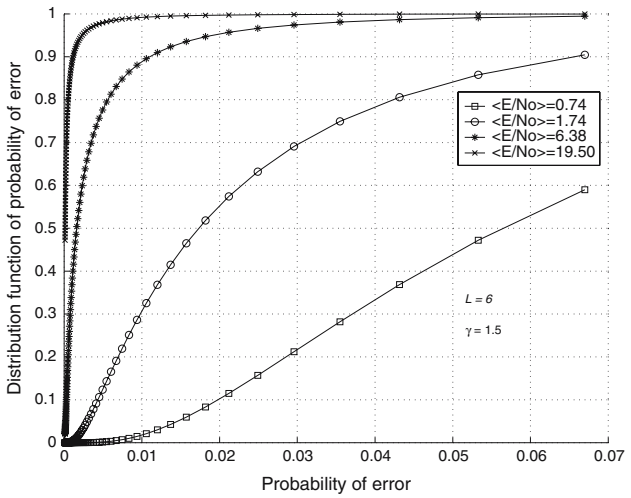

Fig. 4 Cumulative distribution function of the probability of error for a Rician fading with 6-fold diversity for $\left\langle \frac{E(t)}{N_0} \right\rangle = 0.74, 1.74, 6.38, 19.5$, constant $\gamma = 1.5$ and different variances

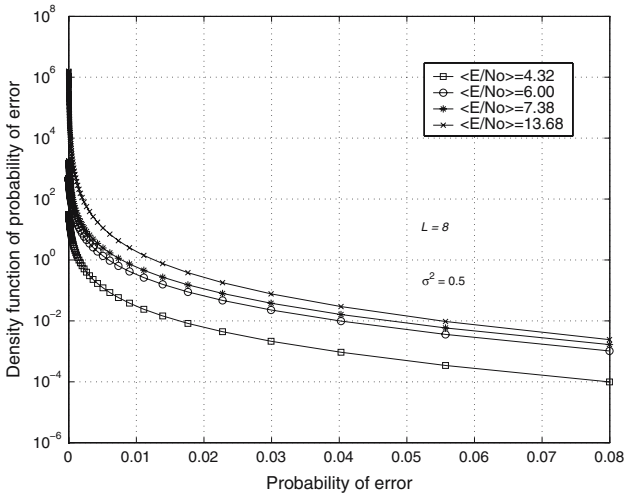

Fig. 6 Density function of the probability of error for a Rician fading channel with 8-fold diversity for $\left\langle \frac{E(t)}{N_0} \right\rangle = 4.32, 6, 7.38, 16.38$, constant variance, $\sigma^2 = 0.5$

5 Conclusion

This paper derives an expression for the signal-to-noise ratio in terms of the received signal amplitudes and phase shifts, transmitted signal, diversity order, signal power and noise spectral density. The error probability distribution and density functions are introduced to characterize the fading process involved in an A-CDMA system. The probability distribution and density functions of the probability of error in an A-CDMA system for Rayleigh and Rician fading channels incorporating diversity, are derived and the results are plotted.

References

1. J. G. Proakis, *Digital Communications*, 4th ed. McGraw Hill, NewYork, 2001.
2. J. Cheng and N. Beaulieu, Accurate DS-CDMA bit-error probability calculation in Rayleigh fading, *IEEE Transactions on Wireless Communications*, Vol. 1, No. 1, pp. 3–15, 2002.
3. S. Choe, C. Georghiades, and K. Narayanan, Improved upper bounds on error probability for biorthogonal trellis-coded CDMA systems, *IEEE Communications Letters*, Vol. 6, No. 9, pp. 361–363, 2002.
4. J. Luo, J. Zeidler, and J. Proakis, Error probability performance for W-CDMA systems with multiple transmit and receive antennas in correlated Nakagami fading channels, *IEEE Transactions on Vehicular Technology*, Vol. 51, No. 6, pp. 1502–1516, 2002.
5. L. Wei and R. Jana, Performance bounds for optimum multiuser DS-CDMA systems. *IEEE Transactions on Communications*, Vol. 47, No. 2, pp. 185–190, 1999.
6. J. Zhang, E. Chong, and D. Tse, Output MAI distributions of linear MMSE multiuser receivers in DS-CDMA systems, *IEEE Transactions on Information Theory*, Vol. 47, No. 3, pp. 1128–1144, 2001.
7. C. Pauw and D. Schilling, Probability of error of M-ary PSK and DPSK on a Rayleigh fading channel, *IEEE Transactions on Communications*, Vol. 36, No. 6, pp. 755–756, 1988.
8. M. Simon and M. Alouini, A unified approach to the probability of error for noncoherent and differentially coherent modulations over generalized fading channels, *IEEE Transactions on Communications*, Vol. 46, No. 12, pp. 1625–1638, 1998.
9. P. Bithas and P. Mathiopoulos, Performance analysis of SSC diversity receivers over correlated Rician fading satellite channels, *EURASIP Journal on Wireless Communications and Networking*, Vol. 2007, No. 1, pp. 53–61, 2007.
10. Q. Zhang, A simple approach to probability of error for equal gain combiners over Rayleigh fading channels, *IEEE Transactions on Vehicular Technology*, Vol. 48, No. 4, pp. 1151–1154, 1999.
11. P. Shankar, Error rates in generalized fading channels, *Journal of Wireless Personal Communications*, Vol. 28, No. 3, pp. 233–238, 2004.
12. Y. Ma, T. Lim, and S. Pasupathy, Error probability for coherent and differential PSK over arbitrary Rician fading channels with multiple cochannel interferers, *IEEE Transactions on Communications*, Vol. 50, No. 3, pp. 429–441, 2002.
13. G. Vitetta, U. Mangali, and D. Taylor, Error probability of FSK incoherent diversity reception with fast Rician fading, *International Journal of Wireless Information Networks*, Vol. 6, No. 2, pp. 107–118, 1999.
14. O. Ugweje, Bit error rate performance of multicarrier CDMA system with application to image transmission. *Journal of Measurement*, Vol. 36, No. 3–4, pp. 233–244, 2004.
15. D. Carey, D. Roviras, and B. Senadji, Approximation of bit error rate distributions for asynchronous multicarrier CDMA and direct-sequence CDMA systems, *Proceedings of the 3rd IEEE International Symposium on Signal processing and Information Technology*, pp. 379–382, 2003.
16. Z. Li and M. Latva-aho, Bit error rate analysis for MC-CDMA systems in Nakagami-*m* fading channels, *EURASIP Journal on Applied Signal Processing*, Vol. 2004, No. 1, pp. 1585–1594, 2004.
17. R. Cameron and B. Woerner, Performance analysis of CDMA with imperfect power control, *IEEE Transactions on Communications*, Vol. 44, No. 7, pp. 777–781, 1996.
18. N. Kong and L. Milstein, Error probability of multicell CDMA over frequency selective fading channels with power control error, *IEEE Transactions on Communications*, Vol. 47, No. 4, pp. 608–617, 1999.
19. V. Bhaskar and L. Joiner, Variable energy adaptation for asynchronous CDMA communications over slowly fading channels, *Journal of Computers and Electrical Engineering*, Vol. 31, pp. 33–55, 2005.
20. G. Lieberman, Adaptive digital communication for a slowly varying channel. *IEEE Transactions on Communication and Electronics*, Vol. 82, No. 65, pp. 44–51, 1963.

Author Biographies

Chen Jie received his Bachelors degree in Telecommunication Engineering in China . He is currently pursuing his Masters degree in the Département Génie des systèmes d'information et de Télécommunication at the Université de Technologie de Troyes, France. His research interests include wireless communications and networking.

Vidhyacharan Bhaskar received the B.Sc. degree in Mathematics from D.G. Vaishnav College, Chennai, India in 1992, M.E. degree in Electrical & Communication Engineering from the Indian Institute of Science, Bangalore in 1997, and the M.S.E. and Ph.D. degrees in Electrical Engineering from the University of Alabama in Huntsville in 2000 and 2002 respectively. During 2002−2003, he was a post-doc fellow with the Communications research group at the University of Toronto. From September 2003 to December 2006, he was an Associate Professor in the Département Génie des systèmes d'information et de Télécommunication at the Université de Technologie de Troyes, France. Since January 2007, he is a Professor and Associate Dean of the School of Electronics and Communications Engineering at S.R.M. University, Kattankulathur, India. His research interests include wireless communications, signal processing, error control coding and queuing theory.